Biosensors and Bioelectronics 182 (2021) 113154

Contents lists available at ScienceDirect

Biosensors and Bioelectronics

journal homepage: http://www.elsevier.com/locate/bios

Electrochemical biosensor for glycine detection in biological fluids

Qianyu Wang [a], Yujie Liu [a], Jonatan C. Campillo-Brocal [b], Amparo Jiménez-Quero [a], Gaston A. Crespo [a], María Cuartero [a,*]

[a] Department of Chemistry, School of Engineering Sciences in Chemistry, Biotechnology and Health, KTH Royal Institute of Technology, Teknikringen 30, SE-100 44, Stockholm, Sweden

[b] Department of Genetics and Microbiology, University of Murcia, Campus Universitario de Espinardo, Murcia, Spain

ARTICLE INFO

Keywords:
Glycine biosensor
Quinoprotein
Prussian blue
Biological fluids
Point-of-care-sensing

ABSTRACT

We present herein the very first amperometric biosensor for the quantitative determination of glycine in diverse biological fluids. The biosensor is based on a novel quinoprotein that catalyzes the oxidation of glycine with high specificity. This process is coupled to the redox conversion of Prussian blue in the presence of hydrogen peroxide originating from the enzymatic reaction. The optimized tailoring of the biosensor design consists of the effective encapsulation of the quinoprotein in a chitosan matrix with the posterior addition of an outer Nafion layer, which is here demonstrated to suppress matrix interference. This is particularly important in the case of ascorbic acid, which is known to influence the redox behavior of the Prussian blue. The analytical performance of the biosensor demonstrates fast response time (<7 s), acceptable reversibility, reproducibility, and stability (<6% variation) as well as a wide linear range of response (25–500 μM) that covers healthy (and even most unhealthy) physiological levels of glycine in blood/serum, urine and sweat. A total of 6 real samples from healthy patients and animals were analyzed: two serum, two urine and two sweat samples. The results were validated *via* commercially available fluorescence kit, displaying discrepancy of less than 9% in all the samples. The unique analytical features and effortless preparation of the new glycine biosensor position it at the forefront of current technologies towards decentralized clinical applications and sport performance monitoring.

1. Introduction

There has been an increasing demand for new point-of-care (POC) tools able to provide trustworthy clinical data in real-time through minimally invasive devices and protocols (Parrilla et al., 2019). Although new analytical methodologies appear daily in the scientific literature, the reality is that only physical parameters (*e.g.* heart rate, respiratory rate, blood pressure and temperature) together with oxygen saturation, glucose, and lactate in blood are routinely analyzed in near-patient circumstances (Guk et al., 2019). Yet, the majority of the clinical information is obtained from collected biological samples, mainly blood, that are analyzed in laboratory equipment (Rosen and Fox 2011). As a result of the absence of versatile tools providing quick, on-site information about patient status, the search for alternative strategies compatible with the POC concept has mainly relied on (bio) sensing research.

In recent years, there has been a remarkable increase in scrutiny paid to amino acids, which are considered to be powerful biomarkers and are present in diverse biological fluids; being saliva, sweat and urine of special interest because they can be accessed through means causing minimal disturbance of the patient (Cuartero et al., 2019; Wu 2010). In particular, glycine, which is the smallest amino acid having only a single hydrogen atom as its side chain, accounts for *ca.*11.5% of total body amino acids and 20% of amino acid nitrogen in body proteins and is known to have a significant association with specific disease states. For example, low plasma glycine levels are related to obesity, diabetes, decreased sleep quality, gout, and schizophrenia, whereas high levels result in nonketotic hyperglycinemia (glycine encephalopathy) (Pérez-Ràfols et al., 2020). Thus, any change or imbalance affecting glycine synthesis and/or catabolism may induce severe syndromes in the individual. Indeed, the amount of glycine endogenously synthetized is not enough to support regular body activity and, hence, dietary intake is crucial to avoid low glycine levels (Meléndez-Hevia et al., 2009). Although incidental glycine insufficiency is not overly detrimental by itself, chronic deficiency may cause severe consequences to organism functioning, such as suboptimal growth and impaired immune response

* Corresponding author.
E-mail address: mariacb@kth.se (M. Cuartero).

https://doi.org/10.1016/j.bios.2021.113154
Received 28 January 2021; Received in revised form 2 March 2021; Accepted 3 March 2021
Available online 11 March 2021

(Jackson 1989). Reviewing the clinical data which has been made available until now makes evident the importance of glycine detection in diagnosis of certain diseases (Pérez-Ràfols et al., 2020).

Today, quantification of glycine in clinical scenarios is restricted to laboratory-based measurements in which the collected sample (usually blood and/or urine) is analyzed using, primarily, liquid chromatography or fluorescence kits (Rosini et al., 2014; Yoshida et al., 2015). While these methods seem to allows for reliable clinical prospects, the time needed for the provision of the results to the physician/nurse/patient ranges from hours to days, as a consequence of sample transportation (to the lab), any required pre-treatments, and the analysis itself, as well as calculations, data delivery and interpretation. In addition, the instrumentation involved necessitates rather significant economic investment, in startup costs, overheads, maintenance, and personnel. Evidently, these constraints would not apply to a POC device for glycine detection.

Having realized the need for alternative analytical methodologies compatible with glycine clinical analysis at the POC level, we have recently reviewed the most prominent biosensors and electrochemical sensors reported for glycine determination in any biological fluid (Pérez-Ràfols et al., 2020). In principle, their inherent features (such as affordability in terms of costs and resources, miniaturization potential, simplicity and robustness) make them unique as the readout in POC configurations, as far as the analytical performances cover the expected physiological ranges of glycine with acceptable selectivity and fast response time. On the other hand, and to the best of our knowledge, none of the reported sensors fulfill the requirements for undiluted biological fluid analysis and most of the approaches lacks appropriate selectivity, linear range of response, and/or capability of measuring at physiological pH, as demonstrated from data collected in that publication (Pérez-Ràfols et al., 2020). As a result, more efforts in the direction of an improved glycine recognition are necessary, likely coming from the introduction of enzyme elements, which totally lacks in the literature (Pérez-Ràfols et al., 2020).

We present herein the very first electrochemical biosensor for glycine detection in any biofluid demonstrating remarkable specificity *via* a quinoprotein with glycine oxidase (GlyOx) activity (Campillo-Brocal et al., 2013). It is here anticipated that the hydrogen peroxide (H_2O_2) produced in the enzymatic reaction is measured owing to its redox activity within the lattice of a Prussian Blue (PB)-based electrode. Upon activation at a constant potential, PB is reduced to Prussian white (PW), which is then oxidized back to PB in the presence of H_2O_2 (Karyakin 2001). In this way an indirect determination of glycine is achieved by the quantification of H_2O_2. We have extensively analyzed the performance of the new glycine biosensor through a series of experiments that provide insights into the working mechanism that dictates the amperometric response of the sensor. We also present an optimized strategy to engineer the quinoprotein-containing sensing element. Advantageously, the new glycine electrochemical biosensor is suitable for the quantification of healthy concentrations of glycine (from 25 to 500 μM) in undiluted serum, urine and sweat (Bouatra et al., 2013; Murphy et al., 2019; Psychogios et al., 2011) with excellent selectivity feature, in contrast to any glycine electrochemical sensor reported up to now (Pérez-Ràfols et al., 2020). The biosensor may also act as an alarm of sorts, in cases where the glycine levels lie outside of this normal range. If necessary, higher glycine concentrations may be more precisely determined by way of sample dilution, in order to fine-tune the clinical analysis.

2. Materials and methods

Details on reagents, materials and instrumentation as well as the protocol for sample analysis are provided in the Supporting Information. The entire fabrication process of the glycine biosensor is illustrated in Fig. S1 and following described. The three electrodes necessary for the amperometric readout were screen-printed over a polyester substrate (12 mm × 12 mm, 0.125 mm thickness), using Carbon ink (C2030519P4, Gwent group, UK) for the working and counter electrodes (WE and CE) and Ag/AgCl ink (C2131007D3, Gwent group, UK) for the reference electrode (RE). Each electrode path consisted of a rectangular part (1.8 × 7.3 mm) with a circular ending (2 mm diameter). This latter zone was further modified in order to obtain the WE, and the electrical connections were established by application of conductive tape to the opposing end of the rectangle. After being screen-printed, the electrode paths were oven-cured at 100 °C for 15 min to induce dehydration. One of the carbon-made electrode paths was then modified to prepare the glycine biosensor by means of three layers: PB mediator, GlyOx-based layer and outer layer. While the recipe for the optimized biosensor tailoring is following provided, notably, the composition of the GlyOx-based layer, the outer layer and the process to immobilize each of the components were systematically optimized and the results are displayed in the results and discussion section.

First, the PB mediator was formed *in situ*, as reported elsewhere (Wiorek et al., 2020), by mixing 15 μL of 0.1 M $FeCl_3$ in 0.01 M HCl solution with 15 μL of 0.1 M potassium ferricyanide $K_3[Fe(CN)_6]$ in 0.01 M HCl solution directly on the electrode surface. This mixture was let stand at room temperature for 10 min, with the exclusion of any incident light, whereafter the vestigial solution was removed using a micropipette. 30 μL of 0.01 M HCl was then added and immediately removed to further clean the modified surface. The PB-modified electrode was again oven-cured at 100 °C for 1 h before subsequent modifications. The original enzyme solution of glycine oxidase labeled as GlyOx (0.96–0.98 U GlyOx/mL) was diluted three times in phosphate buffer. A volume of 2.7 μL of this solution was mixed with 5.4 μL of Chitosan (CHI, 1%, aq.) and the mixture was then drop-cast on top of one PB-modified electrode and allowed to stand for at least 2 h at room temperature until total drying of the layer was achieved. Subsequently, 0.5 μL of a solution of Nafion (prepared by dilution of 0.2 mL of commercial 5% wt. Nafion solution with 0.8 mL of Milli-Q water) was drop-cast on the top of the enzyme film. The modified electrode was kept at room temperature for at least 2 h to dry this last layer, and finally stored in the fridge at 4 °C.

3. Results and discussion

3.1. Initial characterization of the glycine biosensor response

This work demonstrates the very first enzyme-based amperometric biosensor for the detection of glycine in several biological fluids. The flat, miniaturized configuration of the three-electrode system (WE, RE and CE) involved in the electrochemical readout easily allows for different calibration options (see Fig. S2): immersing the electrodes in a recipient with the sample to be measured (referred to as "batch mode" from now on), or by drop casting at least 50 μL of the sample solution onto the surface of the electrodes (the "drop method"). This versatility offers a wide compatibility with different kinds of POC arrangements, in view of further application of the new glycine biosensor for the clinical analysis of any biological fluid. For example, a single drop of blood (or serum) can be analyzed in punctual clinical assays using strips based on the developed sensor. Also, the biosensor could be implemented in microfluidic devices for the continuous monitoring of glycine concentration in urine or sweat (*e.g.,* catheters, epidermal path) as well as microneedle-based sensors prepared by external modification via a layer-by-layer approach, as that herein proposed (García-Guzmán et al., 2020). This adaptability to different calibration paths and scalability into a great plethora of platforms largely exceed the options provided by any glycine electrochemical sensor reported up to now (Pérez-Ràfols et al., 2020).

The electrodes were prepared by immobilizing a series of elements necessary for the appropriate glycine detection. The optimized WE arrangement was found to be composed of a PB mediator layer, a 1:2 v/v mixture of GlyOx:CHI, and finally an outer layer of Nafion in contact with the glycine-containing sample (Fig. 1a). Glycine is expected to diffuse through the Nafion layer and reaching there the GlyOx in the CHI

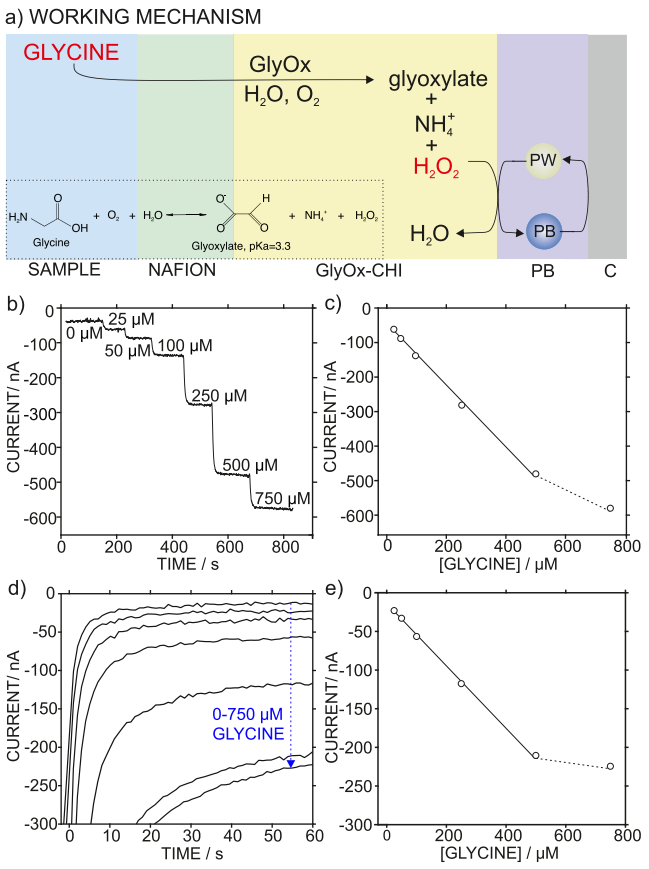

Fig. 1. a) Working mechanism underlaying the response of the glycine biosensor. Amperometric response of the biosensor at increasing concentrations of glycine in artificial serum using **b)** the batch method, with **c)** the corresponding calibration graph and **d)** the drop method, with **e)** the corresponding calibration graph.

matrix. GlyOx, being an oxidase type enzyme, typically gives rise to hydrogen peroxide (H_2O_2) subproduct by enzymatic conversion of glycine in the presence of O_2 (reaction scheme in Fig. 1). The generated H_2O_2 is further reduced while the PW, formed by the reduction of PB upon electrode polarization at −0.05 V, is oxidized back to the original PB form (this occurs spontaneously). Evidently, this working mechanism is analogous to previously reported glucose biosensors based on the PB/PW system (Ricci et al., 2003). While other alternatives have been actively published in the literature regarding the tracing of the generated H_2O_2 (dos Santos Pereira et al., 2019; Raymundo-Pereira et al., 2016; Teixeira et al., 2011), the PB approach seems to be the most widely used.

When developing a universal biosensor for the clinical detection of glycine, the most challenging sample is considered to be blood (or serum) owing to its complex composition. Thus, assessment of the calibration graph in artificial serum may provide information regarding its feasibility towards characterization of such a complex matrix. Fig. 1b shows the dynamic amperometric response of the new glycine biosensor at increasing concentrations of glycine in artificial serum (pH of 7.4) using the batch method, and Fig. 1c presents the corresponding calibration graph. The biosensor displayed a linear response between 25 and 500 µM glycine concentration, with a sensitivity (slope) of 0.881 nA/µM, intercept of −16 nA, limit of detection of 11.1 µM (glycine concentration corresponding to a signal to noise ratio of 3 times the background response and calculated by means of the calibration graph) and response time (the time needed to reach the 90% of the steady-state signal) of < 7s. Above a glycine concentration of 500 µM, the calibration graph starts to deviate from linear behavior. This may be attributed to a typical limitation observed in biosensors whose architecture contains (outer) membranes: the conversion rate of the enzyme reaches a steady state and, therefore, the maximum gradient across the membrane can no longer be sustained. This may result in some accumulation of the substrate at the inner membrane boundary, which is rather undesirable (Bilitewski et al., 1993; Loechel et al., 1998; Schaffar 2002). Nevertheless, the linear response range of the biosensor includes healthy glycine levels, and covers most reported unhealthy concentrations in serum/-blood (Psychogios et al., 2011).

Similar results for the linear range of response (25–500 µM) and the limit of detection (16.4 µM) were observed with the drop method and considering the current reached after a fixed time of 60 s (Fig. 1d and e). However, the slope of the linear calibration graph (0.399 nA/µM) is rather lower than that obtained with the batch method (0.881 nA/µM, Fig. 1c), with an intercept value again in the order of tens of nanoamperes (−8 nA). The lower slope is likely explained by a more efficient mass transport in the case of the batch mode under stirring conditions than is achieved by the drop method (Helm et al., 2010; Moore et al., 2004; Wang and Taha 1991). Also, the time needed to reach the steady-state current seems to depend on the sample matrix. Thus, in phosphate buffer, the steady-state value for the current is reached at just 35 s and, therefore, the calibration graph is not affected by the selected acquisition time whether this time exceeds 35 s (Fig. S3). Notably, it is a common practice to implement a fixed-time amperometric measurement protocol for biosensors working on the "drop-method principle" in order to optimize the time for the sample analysis (Choudhary et al., 2015; Gao et al., 2014; Mi et al., 2019; Zhong et al., 2015).

The working mechanism of the biosensor was next confirmed on the basis of a series of control experiments. First, we tested the response of a naked PB-based electrode at increasing H_2O_2 concentrations using cyclic voltammetry (Fig. 2a) and also, upon polarization at −0.05 V (Fig. 2b) in phosphate buffer background (pH = 7.4). For the cyclic voltammetry experiment, we scanned at 100 mV s^{-1} from −0.5 V to 0.8 V,. In agreement with other reports, the anodic peak appearing at *ca.* 100 mV is ascribed to the PB oxidation while the cathodic peak at −50 mV corresponds to the PB reduction (Karyakin 2001). Note that the peak at *ca.* 750 mV reflects the further PB/Berlin Green transformation (Karyakin 2001). Along with the increasing amount of H_2O_2 in solution (from 0 to 750 µM), a remarkable decrease in the cathodic/anodic peak (with $E_{1/2}$ = 25 mV) was observed. This can be explained as follows: the available PB in its reduced form reaches a maximum in the absence of H_2O_2; therefore, during the anodic and cathodic wave we observe the largest current output (*ca.* 52.3 µA). By contrast, once H_2O_2 is present in the solution, some fraction of PB is spontaneously oxidized, and this translates to a diminishing of the total current output (less PB available for oxidation in the anodic wave).

In the amperometry experiment, the electrode is polarized at −0.05 V covering the PB redox conversion corresponding to the first voltametric peak in the presence of increasing concentration of H_2O_2. The PB electrode presented a linear range of response from 25 to 500 µM, as observed in the inset of Fig. 2b for the batch mode. The explanation for these results may be reasoned as follows. First, in the absence of H_2O_2, the sensor displays a basal current of −1 µA. Then, in the presence of H_2O_2, there is a spontaneous oxidation of the PW formed from the PB electrode at −0.05 V. This re-oxidation of PW to PB results in an increase of the absolute current because of the increasing PB available at the electrode to be reduced to PW. Finally, the absolute current increases with the H_2O_2 concentration because the amount of PW oxidized back to PB increases. Indeed, we found a linear relationship between the measured current and the H_2O_2 concentration in the solution (inset in Fig. 2b), with a slope of 23.20 nA/µM and intercept of −88.2 nA. Note that the observed current levels for electrode calibration were five times lower when using the drop method, in comparison to the batch method (Fig. S4).

Subsequently, the naked PB-based electrode was used to monitor the H_2O_2 formation when glycine was mixed with the GlyOx enzyme at

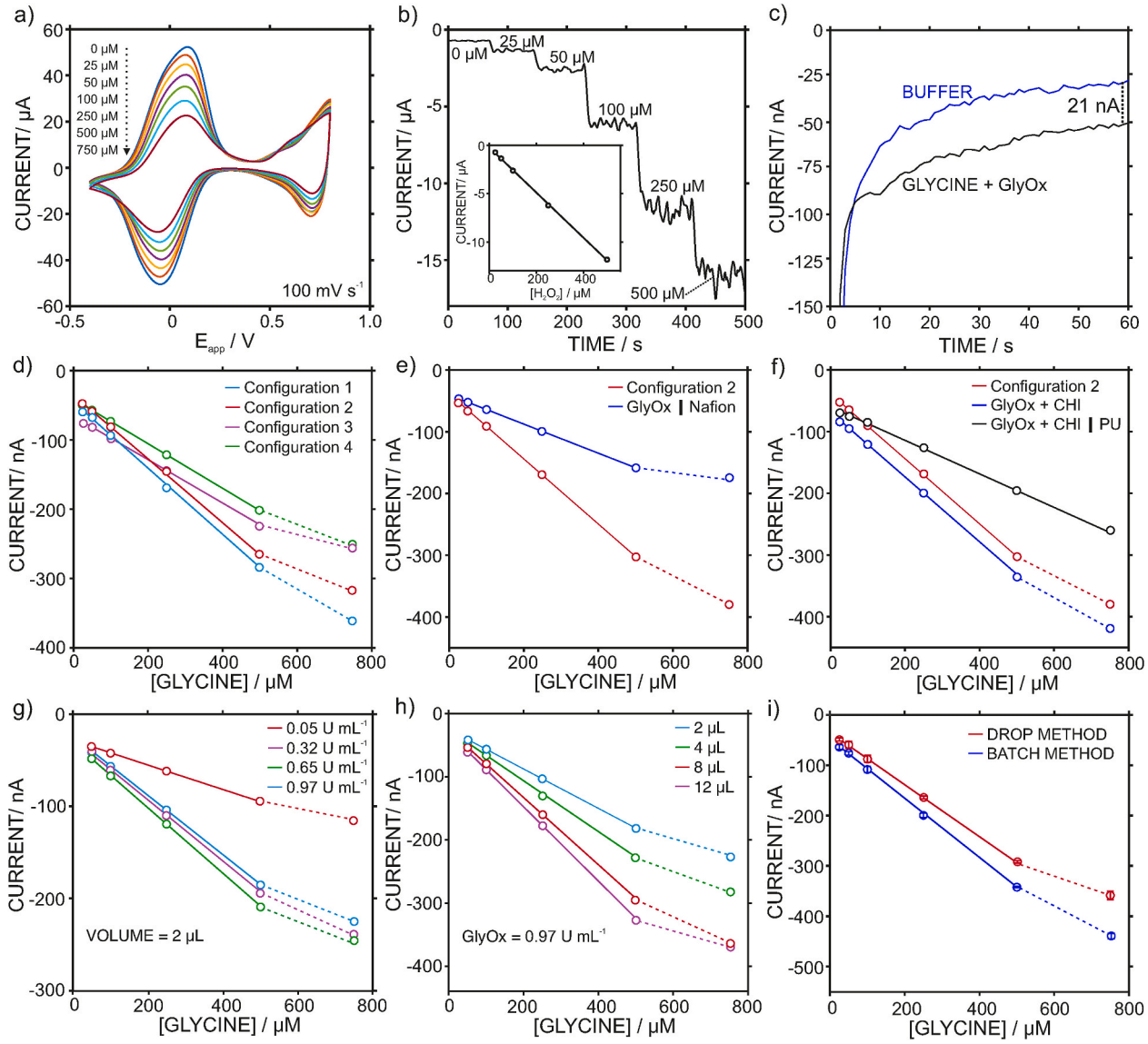

Fig. 2. For the naked PB electrode: **a**) Cyclic voltammograms at increasing H_2O_2 concentrations. Scan rate = 100 mV s^{-1}; **b**) Amperometric response at increasing H_2O_2 concentrations in the batch method. Inset: corresponding calibration graph; **c**) Amperometric response (drop method) in buffer and a mixture of 45 μL of 25 μM glycine plus 5 μL of GlyOx (0.96–0.98 U GlyOx/mL). **d**) Calibration graphs (average of n = 3 electrodes) for different biosensor configurations. **e**) Calibration graphs (n = 3 electrodes) for configuration 2 prepared with and without the GlyOx entrapment in CHI. **f**) Calibration graphs (n = 3 electrodes) for configuration 2 prepared with and without the external Nafion layer, as well as substituting the outer Nafion layer by PU. **g**) Calibration graphs (n = 3 electrodes) at increasing GlyOx concentration in the biosensor using configuration 2 and GlyOx + CHI volume of 2 μL. **h**) Calibration graphs (n = 3 electrodes) for increasing volume of the deposited GlyOx + CHI solution using configuration 2 and enzyme activity of 0.97 U GlyOx mL^{-1}. i) Average of three calibration graphs subsequently accomplished using the same electrode by means of the batch and drop methods. Phosphate buffer (pH = 7.4) was used as the background.

physiological pH (7.4) and utilizing the drop method (Fig. 2c). We mixed 45 μL of 25 μM glycine with 5 μL of GlyOx (0.96–0.98 U GlyOx/mL) and then incubated for 15 min at 37 °C, similar as is recommended in the protocol for the commercially available fluorescence kit for glycine detection. A change of 21 nA in the current was detected: approx. −50 nA for the glycine-enzyme mixture *versus* −29 nA for the buffer medium (basal current). This change is equivalent to the generation of approximately 25 μM concentration of H_2O_2 according to the corresponding calibration graph of the electrode (−71 nA for the glycine-enzyme mixture *versus* −92 nA for the buffer medium, corresponding to a current change of 21 nA, Fig. S4). This result demonstrates that the PB-based electrode can suitably detect the H_2O_2 formed by the quantitative reaction of glycine with the GlyOx-based quinoprotein.

3.2. Optimization of the glycine biosensor response

The optimization of the biosensor response was firstly assessed in terms of tailoring the sensing element. After depositing the PB on the electrode surface, the following configurations were tested: (*Configuration 1*) the GlyOx is entrapped in a matrix composed of CHI and Nafion (60:25:15 GlyOx:CHI:Nafion wt.%); (*Configuration 2*) the GlyOx is immobilized in a CHI matrix (70:30 GlyOx:CHI wt.%) with an outer layer of Nafion on top; (*Configuration 3*) the GlyOx is directly cast on the electrode surface, and then a 60:40 CHI:Nafion wt.% mixture is deposited on top; and (*Configuration 4*) each of the three elements is deposited as an independent layer in the order of GlyOx, CHI and Nafion. The amperometric response of three electrodes of each configuration (n = 3) was obtained at increasing concentrations of glycine in phosphate buffer (pH of 7.4) by means of the drop method. Fig. 2d presents the average

calibration graph for each configuration. No significant differences were observed either by mixing all the components (*configuration 1*) or incorporating the Nafion layer after the GlyOx:CHI mixture (*configuration 2*). Note that a slight change in the intercept of the calibration graph was observed, with sensitivities of 0.477 and 0.458 nA/μM, linear range of response from 25 to 500 μM (in both cases), and limit of detection of 11.6 and 13.7 μM respectively. In all the cases, the variation coefficients for the slope and intercepts (for n = 3 electrodes) were lower than the 5%.

On the other hand, slightly lower sensitivities were observed for the configurations where the enzyme was directly deposited on top of the PB layer followed by the addition of CHI and Nafion, either combined (*configuration 3*) or as separate layers (*configuration 4*), with slopes of 0.312 and 0.321 nA/μM respectively. Indeed, the main impact of the CHI layer was confirmed to be linked to an effective entrapment of the enzyme in consecutive measurements. Thus, Fig. 2e presents the results for a sensor in which CHI was excluded from the preparation recipe. There was a dramatic decrease of the calibration slope down to 0.236 ± 0.019 nA/μM (a change of almost a factor of two in the slope). The sensitivity decreases even more with subsequent calibrations (*ca.* 30% for the second and 15% for the third calibration graph), which likely points out the leaching of the enzyme from the electrode into the solution. This trend is somewhat expected, as it was demonstrated in the literature that CHI provides the appropriate environment for enzyme immobilization, with the entrapment even more effective in systems where the enzyme and CHI exist in a layer sandwiched between the PB and Nafion (Suginta et al., 2013). On the contrary, the presence of the external Nafion layer does not seem to affect the calibration graph accomplished in buffer background: an electrode prepared without this external layer presented similar calibration parameters as those provided with the biosensor prepared with the Nafion outer layer (sensitivity of 0.534 ± 0.106 nA/μM, linear range of response of 25–500 μM, and limit of detection of 9.02 μM, see blue line in Fig. 2f).

Interestingly, substitution of the Nafion layer with polyurethane (PU), which was selected to provide enhanced biocompatibility in polymer-based electrochemical sensors (Cuartero et al., 2016), resulted in the widening of the linear range of response while reducing the biosensor sensitivity (slope of 0.265 nA/μM), with the saturation of the GlyOx appearing at a higher glycine concentration (750 μM for Nafion *versus* 1000 μM for PU). This behavior can likely be explained by the lower glycine partitioning displayed by PU than Nafion and, which results in a lower concentration of glycine reaching the enzyme (Kataky et al., 2002). Incorporation of a PU layer could therefore be used as a strategy to expand the linear range of response, while sacrificing some sensitivity of the biosensor. This technique may prove useful when, for example, analyzing samples with uncommonly high glycine levels arising from certain diseases. A particularly applicable use for this biosensor would be sweat analysis while practicing sport; elevated glycine concentrations have been reported under these conditions (Murphy et al., 2019).

Next, we investigated the effect on the biosensor response of the amount of enzyme deposited, by changing both the concentration and the volume used in *configuration 2*, with the GlyOx immobilized in a CHI matrix and a Nafion layer on top (n = 3 electrodes in all the calibration graphs). Fig. 2g and h show the obtained calibration graphs. First, different enzyme activities of the GlyOx (obtained by dilution by a factor of 18, 3, and 1.5, as well as no dilution, of the original enzyme solution of 0.97 ± 0.01 U GlyOx mL^{-1} in phosphate buffer, corresponding to 0.05, 0.32, 0.65 and 0.97 U GlyOx mL^{-1} respectively) were tested while keeping the total deposited volume constant at 2 μL (1 μL of GlyOx + 1 μL of CHI). At lower enzyme activity, an increase in the enzyme activity caused an increase in the biosensor sensitivity (from 0.134 ± 0.009 to 0.322 ± 0.040 nA/μM using 0.05 and 0.32 U GlyOx mL^{-1} respectively), while keeping the intercept close to −50 nA. This sensitivity was then approximately constant for higher enzyme activities (0.354 ± 0.018 and 0.314 ± 0.060 nA/μM, for 0.65 and 0.97 U GlyOx mL^{-1} respectively). The linear range of response was the same (25–500 μM) in all cases. Nevertheless, according to the results shown in Fig. 2g, a GlyOx activity between 0.65 and 0.95 U GlyOx mL^{-1} is sufficient for the biosensor to show acceptable sensitivity.

Considering an activity of 0.65 U GlyOx mL^{-1}, the calibration graphs observed for varying volumes of deposited GlyOx solution are shown in Fig. 2h. The sensitivity was found to dramatically increase with the volume of deposited enzyme solution: 0.314 ± 0.060, 0.405 ± 0.033 and 0.535 ± 0.072 nA/μM, using 2, 4 and 8 μL respectively. This increase was less perceptible when increasing the volume from 8 to 12 μL (0.593 ± 0.151 nA/μM), with the linear range of response remaining constant throughout (25–500 μM). Accordingly, and considering also the results observed at varying the GlyOx concentration, a volume of 8 μL and activity of 0.65 U GlyOx mL^{-1} were decided upon for use in *configuration 2*.

3.3. Evaluation of the analytical performance of glycine biosensors

Fig. 2i presents the average graph obtained as a result of three consecutive calibrations using the same electrode by means of the batch and drop methods. In both cases, the variation coefficient for the slope was rather low (4% for the batch mode and 3% for the drop method), with a slightly higher sensitivity observed for the batch mode (0.575 nA/μM *versus* 0.532 nA/μM), as well as similar linear range of response (25–500 μM) and intercepts (−35.9 ± 4.2 nA *versus* −48.4 ± 4.5 nA). Analogous results were observed for the reproducibility of the amperometric response corresponding to 5 different biosensors (Fig. 3a), with variation coefficients of 5% and 2% for the slopes of the batch and drop methods respectively. Furthermore, the intercept variations were more than acceptable taking into consideration uncertainties associated with the (hand-made) layer-by-layer fabrication technique of the biosensor (2% and 4% for the batch and drop methods respectively). The limit of detection (14.5 μM for the batch method and 17.6 μM for the drop method), and linear range of response (25–500 μM) were practically the same no matter the calibration method used.

The reversibility was found to be excellent, as observed in Fig. 3b for two complete calibration graphs by means of the drop method and in Fig. 3c for the sequence of 50→500→50→500→50→500 μM glycine concentration. In particular, for the complete calibration graph, slope and intercept of 0.532 ± 0.01 nA/μM and −28.4 ± 4.5 nA were observed. Then, for the concentration sequence, a variation in the current response of 0.7% for 50 μM and 1.5% for 500 μM glycine was observed, which corresponds to a maximum error of *ca.* 5% in the quantitative provision of 50 and 500 μM glycine concentration. The signal drift was studied for additions of 25 and 500 μM glycine over phosphate buffer background (Fig. 3d), resulting in negligible magnitudes of 1.6 and 3.3 nA/h respectively. Furthermore, the lifetime and stability of the sensor were evaluated under different conditions, as detailed in the Supporting Information. Essentially, the biosensor can be continuously used over a month after preparation and storing it in the fridge, immersed in a 50 μM glycine solution. The sensitivity of the biosensor was found to have decreased by 6% on the 5th day, and 35% on the 30th day of continuous usage. These variations in the sensitivity (slope) can be thoroughly circumvented by daily recalibration of the biosensor, as the linear range of response and limit of detection (8–10 μM) are well maintained.

Fig. 4a presents calibration graphs obtained at various pH in the background solution. These calibration graphs are almost superposed, showing only very small variations in sensitivity (Table S1) and exactly the same linear range of response (25–500 μM). As a result, we anticipate no influence of the pH of the sampling medium on the amperometric response of the new glycine biosensor. Moreover, we did not observe any drastic influence of T on the biosensor response, beyond a very slight change in the initial current of the baseline. Fig. 4b shows the calibration graphs at different temperatures. It can be seen that variation of the temperature causes no significant effect upon the sensitivity nor

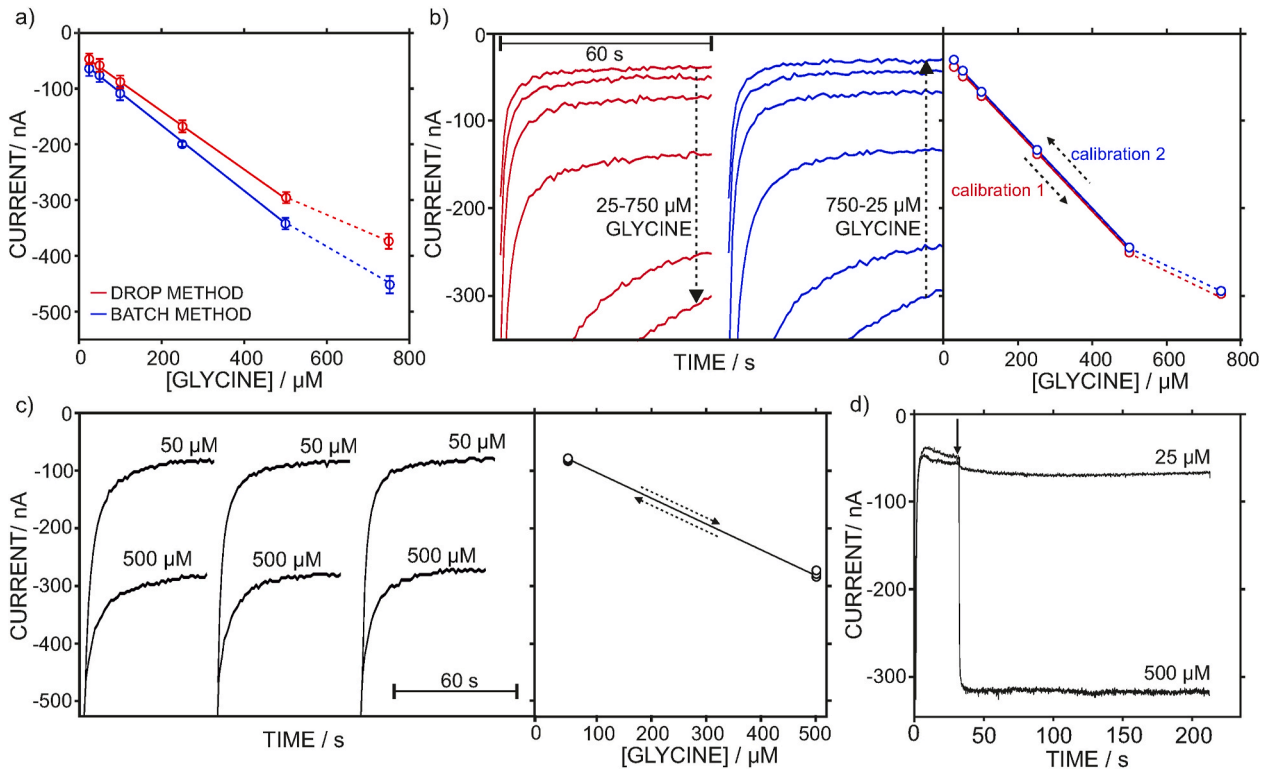

Fig. 3. **a**) Average calibration graph with five electrodes using the batch and drop methods. **b**) Reversibility of the complete calibration graph using the drop method. Left: Dynamic amperometric response. Right: corresponding calibration graphs. Arrows indicate the direction of the measurements. **c**) Reversibility of the biosensor response following the sequence 50→500→50→500→50→500 μM glycine concentration in the drop method. Left: Dynamic amperometric response. Right: corresponding calibration graphs. Arrows indicate the direction of the measurements. **d**) Long-term amperometric response of 25 and 500 μM glycine concentrations for 200 s in the drop method. The arrow indicates the glycine addition in the phosphate buffer background.

the linear range of response of the biosensor (Table S1). A further experiment was carried out wherein the entire calibration graph was recorded while induced drastic changes in temperature from 20 °C to 40 °C and back again to 20 °C. Once again, the biosensor did not present any change in its sensitivity, displaying a variation of 1% from 20 °C to 40 °C, 5% from 40 °C to 20 °C, and a variation of 4% comparing the calibration at 20 °C before and after increasing the temperature to 40 °C (Table S1).

3.4. Interference study

The concentrations tested in the interference study were always higher than those expected in the real biofluids (Bouatra et al., 2013; Murphy et al., 2019; Psychogios et al., 2011). The following species produced negligible variation in the biosensor response, both in background solution and in 250 μM glycine solution: 5 mM KCl, 1 mM $MgCl_2$, 5 mM urea, 10 mM uric acid, 5 mM glucose, 5 mM creatinine, 100 mM creatine, 150 mM NaCl, 5 mM $CaCl_2$, 250 μM lactate, 250 μM pyruvate, 250 μM $FeCl_3$, 250 μM ascorbic acid (Fig. 4d). Of special interest is the case for ascorbic acid because, as previously reported in the literature, it can be directly oxidized in the PB lattice (Castro et al., 2001; Zloczewska et al., 2014). Advantageously, ascorbic acid interference is avoided using the biosensor prepared with an external layer of Nafion: the calibration graph for glycine is exactly the same in the presence and absence of ascorbic acid (Fig. 4c versus Fig. 4d). By contrast, if this layer is omitted during the biosensor fabrication, the entire calibration graph shifts to higher current values (Fig. S5). Whether this plot is used to quantify glycine content in an unknown sample, the result would be an underestimate of the true concentration. Notably, other substances prone to be present in the different biological fluids (such as amino acids and related compounds, e.g., dopamine, as well as hormones) were not included in the present study because these have been already demonstrated not to interfere with the GlyOx enzyme and/or the redox behavior of the PB (Campillo-Brocal et al., 2013; Matos-Peralta and Antuch 2019; Wiorek et al., 2020). Moreover, the selectivity study could be further extended to specific drugs considering the application of the developed glycine biosensor to the tracing of particular diseases in which patients are under controlled clinical treatments.

Biosensors prepared following recipes other than the external-Nafion-layer-based configuration 2 displayed certain interference from ascorbic acid, despite otherwise presenting good analytical performances. Fig. S6 presents the biosensor response towards a sequence of additions involving buffer, 500 μM glycine and 250 μM of ascorbic acid. First of all, the response of the biosensor prepared with an external PU layer presented lower sensitivity overall. Then, the three biosensors presented a decrease in current when ascorbic acid was added; that is to say that PW/PB conversion at the electrode surface is less prominent (see Fig. 1a). In terms of errors, in all the cases the glycine concentration provided by the biosensor will be lower than the real value, *e.g.,* when detecting 500 μM of glycine, errors of approximately 30–50% will be obtained. As a result, the use of an external Nafion layer is advised to avoid the interference of ascorbic acid.

3.5. Validated analysis of glycine content in serum, urine and sweat samples

Fig. 5 shows glycine calibrations in artificial urine, sweat and serum background, noting that the dynamic curves were already shown in Fig. 1 in the case of serum. We could not appreciate any matrix interference in the obtained calibrations (Table S2). Indeed, any change in the calibration is likely attributed to the between-electrode variation of the developed biosensor rather than any matrix effect. Similar to what was observed in phosphate buffer background, the sensitivity in the case of the batch method is always higher than it is when using the drop

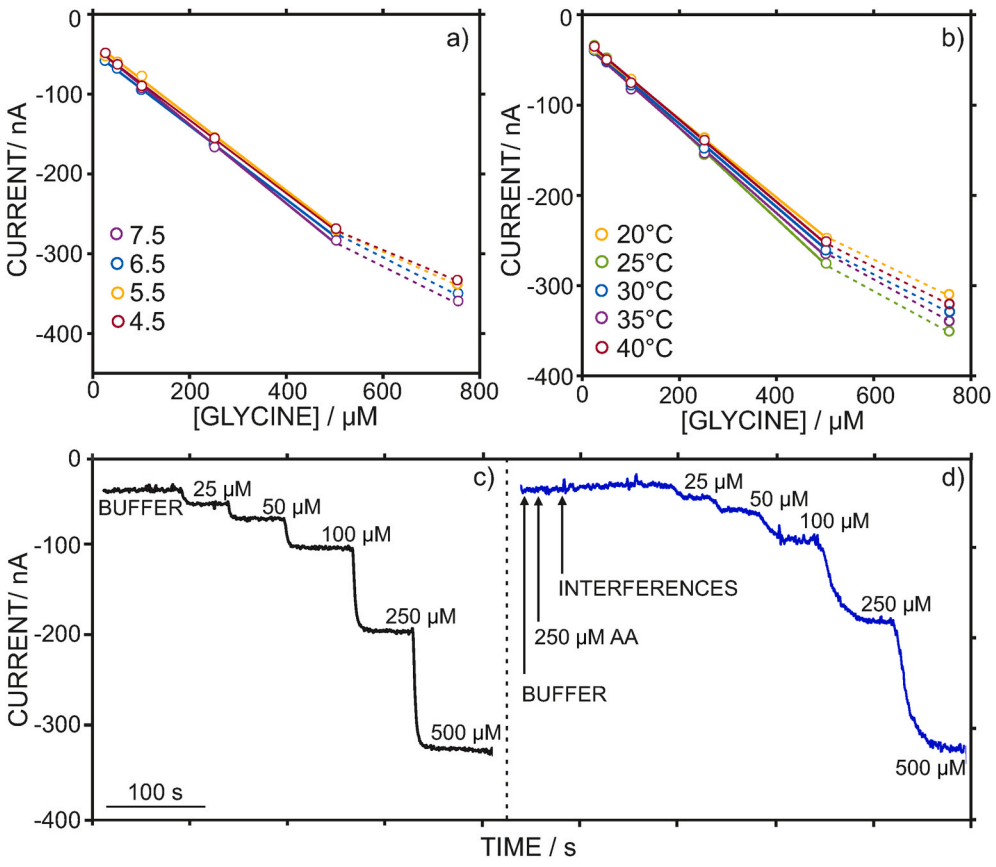

Fig. 4. **a**) Calibration graphs at different pH using the drop method. **b**) Calibration graphs at different temperatures using the batch mode. **c**) Amperometric response at increasing glycine concentration in buffer background (batch mode). **d**) Dynamic response at increasing glycine concentration after adding to the background solution (phosphate buffer at pH of 7.4): i) 250 μM of ascorbic acid (AA) and ii) interferences: 5 mM KCl, 1 mM $MgCl_2$, 5 mM urea, 5 mM glucose, 5 mM creatinine, 100 mM creatine, 150 mM NaCl, 5 mM $CaCl_2$, 250 μM lactate, 250 μM pyruvate and 250 μM of $FeCl_3$ (batch mode).

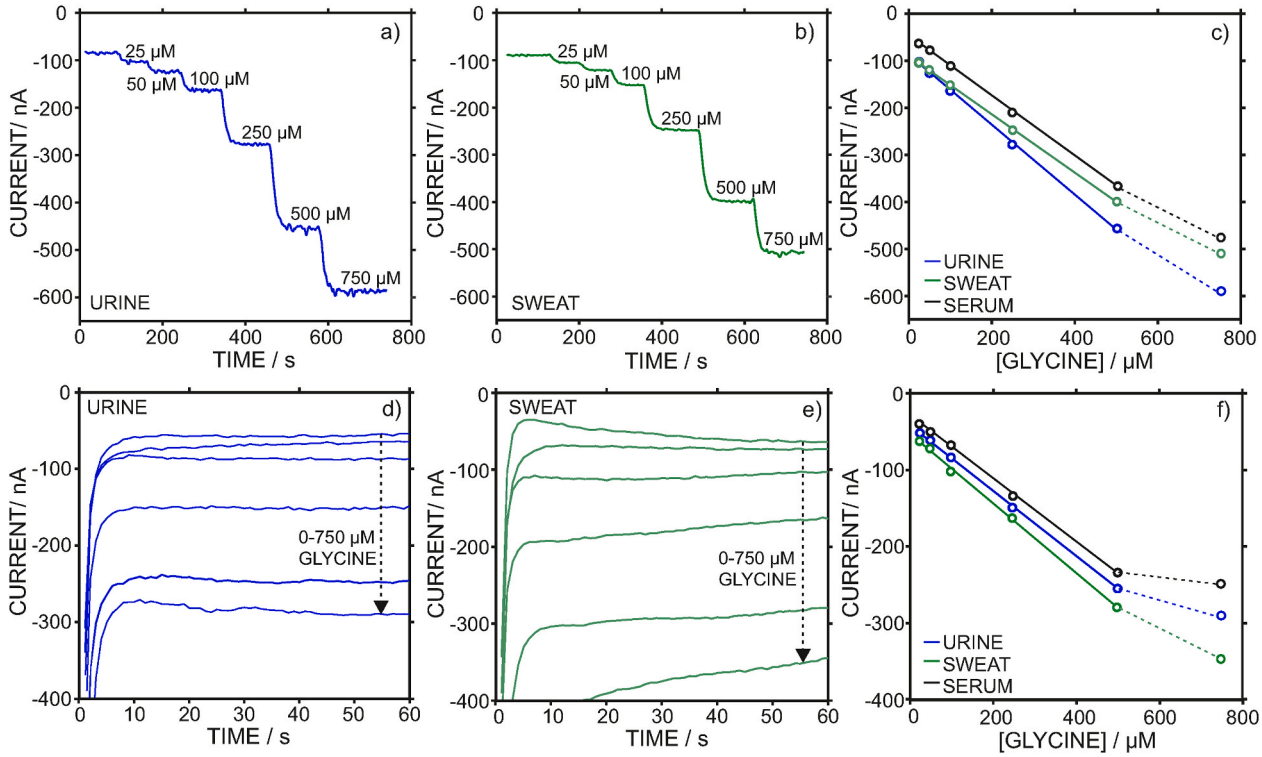

Fig. 5. **a**) Amperometric response at increasing glycine concentrations in artificial urine (batch method). **b**) Amperometric response at increasing glycine concentrations in artificial sweat (batch method). **c**) Calibration graphs obtained in artificial urine, sweat and serum with the batch method. **d**) Amperometric response at increasing glycine concentrations in artificial urine (drop method). **e**) Amperometric response at increasing glycine concentrations in artificial sweat (drop method). **f**) Calibration graphs obtained in artificial urine, sweat and serum with the drop method.

method (see Table S2). Overall, these results highlight the potential of the new biosensor for use in the detection of glycine in any biological fluid, with the implementation of calibration in the concentration range 25–500 μM.

Table 1 collects the results for glycine detection in several real samples (2 serum, 2 sweat and 2 urine samples) obtained using both the new biosensor (drop method) and the commercial kit for fluorescence detection. Notably, the use of the drop method reduces the needed sample volume down to 50 μL, which is very convenient to avoid the requirement of a high sample volume from the patient. In all the cases, the difference in glycine concentrations provided by the two techniques is lower than 9%. In addition, the observed glycine levels were in accordance with those reported in the literature for each biological fluid. For example, Peters and co-workers found levels of *ca.* 400–500 μM of glycine in horse serum, whereas Baetz et al. reported glycine levels of approximately 600 μM in fetal bovine serum (Baetz et al., 1975; Peters et al., 2013). Then, Murphy et al. presented glycine levels in sweat of *ca.* 1750 μM in passive conditions, with this amount gradually diminishing to approximately 600 μM with controlled exercise (Murphy et al., 2019). Dunstan and co-workers reported levels of around 900 μM after practicing exercise (Dunstan et al., 2016). Regarding urine, glycine levels are commonly related to the concentration of urine creatinine, and normal values fall in the range of 50–300 μM glycine/mM creatinine (Bouatra et al., 2013). Overall, the biosensor provides highly accurate results and these are included in normal glycine levels in each biological fluid, which is one key advantage over any glycine electrochemical sensor reported up to now (Pérez-Ràfols et al., 2020).

Table 1
Glycine levels detected in different biological fluid samples by means of the developed biosensor and the fluorescence kit.

Sample	Commercial kit (μM)	Biosensor (μM)	% Difference
Horse serum	414 ± 9	419 ± 9	1.2
Fetal bovine serum	493 ± 5	469 ± 6	4.9
Sweat 1[c]	918 ± 7	1004[d]	9.3
Sweat 2[c]	940 ± 11	907[d]	3.5
Urine 1	331 ± 5[a]	357 ± 8	7.9
Urine 2	471 ± 3[b]	479 ± 2	1.7

[a] 77.5 μM Glycine/mM creatinine.
[b] 184.4 μM Glycine/mM creatinine.
[c] The sample was diluted prior to the analysis with the biosensor.
[d] Only one measurement was accomplished because of the low sample volume.

4. Conclusions

The very first amperometric biosensor for glycine detection in several biological fluids is presented herein. The biosensor is tailored to a new design that allows for the specific and selective detection of glycine owing to the incorporation of a novel quinoprotein in chitosan matrix with a Nafion layer on top. The analytical principle is combined with the redox conversion of Prussian blue in the presence of hydrogen peroxide (generated by the enzymatic reaction) assisted by the quinoprotein, which is exclusive for glycine as substrate. The performance of the biosensor was exhaustively evaluated, showing a fast response time, good reversibility, reproducibility and stability, as well as a linear range of response that covers healthy (and even most unhealthy) physiological levels of glycine in blood/serum, urine and sweat. In addition, ascorbic acid did not represent any interference in the biosensor response, in contrast to other Prussian blue electrodes. Real serum, sweat and urine samples were analyzed with the new glycine biosensor and by means of a commercially available fluorescence kit. The results showed differences of less than 9% for all samples. All the results presented in this paper position the new glycine biosensor at the forefront of current analytical advances towards a POC device for clinical applications and sport performance monitoring for wellbeing.

CRediT authorship contribution statement

Qianyu Wang: Data curation, Formal analysis, Investigation, Methodology, Software, Validation, Visualization, Writing – original draft. **Yujie Liu:** Methodology, Software, Validation, Visualization, Writing – review & editing. **Jonatan C. Campillo-Brocal:** Conceptualization, Methodology, Writing – review & editing. **Amparo Jiménez-Quero:** Methodology, Validation, Writing – review & editing. **Gaston A. Crespo:** Conceptualization, Funding acquisition, Methodology, Resources, Supervision, Visualization, Writing – original draft. **María Cuartero:** Conceptualization, Data curation, Formal analysis, Funding acquisition, Investigation, Methodology, Project administration, Resources, Software, Supervision, Validation, Visualization, Writing – original draft, Writing – review & editing, All authors discussed the results and contributed to the final manuscript. All authors have approved the final version to be published.

Declaration of competing interest

The authors declare that they have no known competing financial interests or personal relationships that could have appeared to influence the work reported in this paper.

Acknowledgments

This project has received funding from the European Union's Horizon 2020 research and innovation programme under Marie Skłodowska-Curie grant agreement No. 792824. M.C. acknowledges the support from the Swedish Research Council (VR-2019-04142). G.A.C. gratefully thanks KTH Royal Institute of Technology (K-2017-0371) and the Swedish Research Council (Project Grant VR-2017–4887). Q.W. and Y.L. gratefully thank the China Scholarship Council for supporting their PhD. studies. We thank Prof. Per Berglund for allowing the use of lab premises to synthetize the quinoprotein and Dr. Rocio Canovas for some initial guidance in this project.

Appendix A. Supplementary data

Supplementary data to this article can be found online at https://doi.org/10.1016/j.bios.2021.113154.

References

Baetz, A., Hubbert, W., Graham, C., 1975. Reproduction 44 (3), 437–444.
Bilitewski, U., Jäger, A., Rüger, P., Weise, W., 1993. Sensor. Actuator. B Chem. 15 (1–3), 113–118.
Bouatra, S., Aziat, F., Mandal, R., Guo, A.C., Wilson, M.R., Knox, C., Bjorndahl, T.C., Krishnamurthy, R., Saleem, F., Liu, P., 2013. PloS One 8 (9), e73076.
Campillo-Brocal, J.C., Lucas-Elio, P., Sanchez-Amat, A., 2013. Microbiologyopen 2 (4), 684–694.
Castro, S.S., Balbo, V.R., Barbeira, P.J., Stradiotto, N.R., 2001. Talanta 55 (2), 249–254.
Choudhary, T., Rajamanickam, G., Dendukuri, D., 2015. Lab Chip 15 (9), 2064–2072.
Cuartero, M., Crespo, G.A., Bakker, E., 2016. Anal. Chem. 88 (11), 5649–5654.
Cuartero, M., Parrilla, M., Crespo, G.A., 2019. Sensors 19 (2), 363.
dos Santos Pereira, T., de Oliveira, G.C.M., Santos, F.A., Raymundo-Pereira, P.A., Oliveira Jr., O.N., Janegitz, B.C., 2019. Talanta 194, 737–744.
Dunstan, R.H., Sparkes, D.L., Dascombe, B.J., Macdonald, M.M., Evans, C.A., Stevens, C. J., Crompton, M.J., Gottfries, J., Franks, J., Murphy, G., 2016. PloS One 11 (12), e0167844.
Gao, Z.-D., Qu, Y., Li, T., Shrestha, N.K., Song, Y.-Y., 2014. Sci. Rep. 4, 6891.
García-Guzmán, J.J., Pérez-Ràfols, C., Cuartero, M., Crespo, G.A., 2020. TrAC Trends Anal. Chem. 135, 116148.
Guk, K., Han, G., Lim, J., Jeong, K., Kang, T., Lim, E.-K., Jung, J., 2019. Nanomaterials 9 (6), 813.
Helm, I., Jalukse, L., Leito, I., 2010. Sensors 10 (5), 4430–4455.
Jackson, A.A., 1989. Proc. Nutr. Soc. 48 (2), 293–301.
Karyakin, A.A., 2001. Prussian blue and its analogues: electrochemistry and analytical applications. Electroanalysis 13 (10), 813–819.
Kataky, R., Bryce, M., Goldenberg, L., Hayes, S., Nowak, A., 2002. Talanta 56 (3), 451–458.
Loechel, C., Chemnitius, G.-C., Borchardt, M., Cammann, K., 1998. Z. Lebensm. Unters. Forsch. A 207 (5), 381–385.

Matos-Peralta, Y., Antuch, M., 2019. J. Electrochem. Soc. 167 (3), 037510.
Meléndez-Hevia, E., de Paz-Lugo, P., Cornish-Bowden, A., Cárdenas, M.L., 2009. J. Biosci. 34 (6), 853–872.
Mi, S., Xia, J., Xu, Y., Du, Z., Sun, W., 2019. RSC Adv. 9 (16), 9006–9013.
Moore, E.J., Kreuzer, M.P., Pravda, M., Guilbault, G.G., 2004. Electroanalysis 16 (20), 1653–1659.
Murphy, G.R., Dunstan, R.H., Macdonald, M.M., Borges, N., Radford, Z., Sparkes, D.L., Dascombe, B.J., Roberts, T.K., 2019. PloS One 14 (10), e0223381.
Parrilla, M., Cuartero, M., Crespo, G.A., 2019. Trac. Trends Anal. Chem. 110, 303–320.
Pérez-Ràfols, C., Liu, Y., Wang, Q., Cuartero, M., Crespo, G.A., 2020. Sensors 20 (14), 4049.
Peters, L., Smiet, E., de Sain-van der Velden, M., van der Kolk, J., 2013. Vet. Q. 33 (1), 20–24.
Psychogios, N., Hau, D.D., Peng, J., Guo, A.C., Mandal, R., Bouatra, S., Sinelnikov, I., Krishnamurthy, R., Eisner, R., Gautam, B., 2011. PloS One 6 (2), e16957.
Raymundo-Pereira, P.A., Shimizu, F.M., Coelho, D., Piazzeta, M.H., Gobbi, A.L., Machado, S.A., Oliveira Jr., O.N., 2016. Biosens. Bioelectron. 86, 369–376.
Ricci, F., Amine, A., Palleschi, G., Moscone, D., 2003. Biosens. Bioelectron. 18 (2–3), 165–174.
Rosen, S., Fox, M.P., 2011. PLoS Med. 8 (7), e1001056.
Rosini, E., Piubelli, L., Molla, G., Frattini, L., Valentino, M., Varriale, A., D'Auria, S., Pollegioni, L., 2014. FEBS J. 281 (15), 3460–3472.
Schaffar, B.P., 2002. Anal. Bioanal. Chem. 372 (2), 254–260.
Suginta, W., Khunkaewla, P., Schulte, A., 2013. Chem. Rev. 113 (7), 5458–5479.
Teixeira, M.F., Cincotto, F.H., Raymundo-Pereira, P.A., 2011. Electrochim. Acta 56 (19), 6804–6811.
Wang, J., Taha, Z., 1991. Anal. Chem. 63 (10), 1053–1056.
Wiorek, A., Parrilla, M., Cuartero, M., Crespo, G.n.A., 2020. Anal. Chem. 92 (14), 10153–10161.
Wu, G., 2010. Adv. Nutr. 1 (1), 31–37.
Yoshida, H., Kondo, K., Yamamoto, H., Kageyama, N., Ozawa, S.-i., Shimbo, K., Muramatsu, T., Imaizumi, A., Mizukoshi, T., Masuda, J., 2015. J. Chromatogr. B 998, 88–96.
Zhong, G., Lan, R., Zhang, W., Fu, F., Sun, Y., Peng, H., Chen, T., Cai, Y., Liu, A., Lin, J., 2015. Int. J. Nanomed. 10, 2219.
Zloczewska, A., Celebanska, A., Szot, K., Tomaszewska, D., Opallo, M., Jönsson-Niedziolka, M., 2014. Biosens. Bioelectron. 54, 455–461.